2001

Middle-Ear Function with Tympanic-Membrane Perforations. II. A Simple Model.

Susan E. Voss
Smith College, svoss@smith.edu

John J. Rosowski
Harvard Medical School

Saumil N. Merchant
Harvard Medical School

William T. Peake
Massachusetts Eye and Ear Infirmary

Middle-ear function with tympanic-membrane perforations. II. A simple model

Susan E. Voss[a)]
Picker Engineering Program, Smith College, 51 College Lane, Northampton, Massachusetts 01063; Eaton-Peabody Laboratory of Auditory Physiology and Department of Otolaryngology, Massachusetts Eye and Ear Infirmary, Boston, Massachusetts 02114; Speech and Hearing Sciences Program, Harvard–M.I.T. Division of Health Sciences and Technology, Cambridge, Massachusetts 02139; Department of Otology and Laryngology, Harvard Medical School, Boston, Massachusetts; and Research Laboratory of Electronics, Massachusetts Institute of Technology, Cambridge, Massachusetts 02139

John J. Rosowski
Eaton-Peabody Laboratory of Auditory Physiology and Department of Otolaryngology, Massachusetts Eye and Ear Infirmary, Boston, Massachusetts 02114; Speech and Hearing Sciences Program, Harvard–M.I.T. Division of Health Sciences and Technology, Cambridge, Massachusetts 02139; Department of Otology and Laryngology, Harvard Medical School, Boston, Massachusetts; and Research Laboratory of Electronics, Massachusetts Institute of Technology, Cambridge, Massachusetts 02139

Saumil N. Merchant
Eaton-Peabody Laboratory of Auditory Physiology and Department of Otolaryngology, Massachusetts Eye and Ear Infirmary, Boston, Massachusetts 02114; Speech and Hearing Sciences Program, Harvard–M.I.T. Division of Health Sciences and Technology, Cambridge, Massachusetts 02139; and Department of Otology and Laryngology, Harvard Medical School, Boston, Massachusetts 02114

William T. Peake
Eaton-Peabody Laboratory of Auditory Physiology and Department of Otolaryngology, Massachusetts Eye and Ear Infirmary, Boston, Massachusetts 02114; Speech and Hearing Sciences Program, Harvard–M.I.T. Division of Health Sciences and Technology, Cambridge, Massachusetts 02139; and Department of Electrical Engineering and Computer Science and Research Laboratory of Electronics, Massachusetts Institute of Technology, Cambridge, Massachusetts 02139

(Received 27 December 2000; revised 1 March 2001; accepted 24 May 2001)

A quantitative model of the human middle ear with a tympanic-membrane (TM) perforation is developed. The model is constrained by several types of acoustic measurements made on human cadaver ears, which indicate that perforation-induced changes in transmission result primarily from changes in driving pressure across the TM and that perforation-induced change in the structure of the TM and its coupling to the ossicles contributes a substantially smaller component. The model represents the effect of a perforation on the pressure difference across the TM by inclusion of a path for sound coupling through the perforation from the ear canal to the middle-ear cavity. The model implies that hearing loss with perforations depends primarily on three quantities: the perforation diameter, sound frequency, and the volume of air in the middle-ear cavity. For the conditions that produce the largest hearing loss (low frequency and large perforation), the model yields a simple dependence of loss on frequency, perforation diameter, and middle-ear cavity volume. Predictions from this model may be useful to clinicians in determining whether, in particular cases, hearing losses are explainable by the observed perforations or if additional pathology must be involved. [DOI: 10.1121/1.1394196]

PACS numbers: 43.64.Ha, 43.64.Bt, 43.70.Bk, 43.70.Gr [BLM]

I. INTRODUCTION

Measured effects of tympanic-membrane (TM) perforations on sound transmission through the middle ear have been systematically described (Voss *et al.*, 2001d). The measurements indicate that, for perforations up to half the area of the TM, the major mechanism for perforation-induced changes is an altered pressure difference across the TM. In this paper we develop a measurement-based mathematical model that describes sound transmission in ears with perforations. The model assumes that the effect of the perforation on the pressure difference across the TM can be represented by inclusion of a path for sound coupling through the perforation from the ear canal to the middle-ear cavity. The properties of this path are described by an impedance. The primary goal of this paper is to test whether this simple model represents features of the measurements.

[a)]Author to whom correspondence should be addressed. Address for correspondence: Smith College, Picker Engineering Program, 51 College Lane, Northampton, MA 01063; electronic mail: svoss@email.smith.edu

II. MIDDLE-EAR ANALOG CIRCUIT MODEL WITH TM PERFORATIONS

A. Circuit topology

The equations that govern sound pressures and volume velocities in acoustic systems are analogous to the equations that describe voltages and currents in electric circuits. Here, we use an analog-circuit model (Fig. 1) to represent the middle ear with a TM perforation. To distinguish them from measurements, model values are indicated with a circumflex above the variable. The perforation is represented by a volume-velocity path of impedance $\hat{Z}_{\text{perf}}$ from the ear-canal side of the TM to the middle-ear cavity. $\hat{Z}_{\text{perf}}$ depends on the size of the perforation; when there is no perforation, $|\hat{Z}_{\text{perf}}|$ is infinite, and the middle-ear cavity impedance $\hat{Z}_{\text{cav}}$ is in series with an impedance $\hat{Z}_{\text{TOC}}$ that represent the effects of the TM, ossicles, and cochlea (as in, e.g., Onchi, 1961; Møller, 1961; Zwislocki, 1962; Kringlebotn, 1988; Peake *et al.*, 1992; Shera and Zweig, 1992; Whittemore *et al.*, 1998).

The impedance $\hat{Z}_{\text{TOC}}$ is the input impedance of the two-port network, representing the coupling of sound through the TM and ossicles, terminated by an impedance that represents the stapes and cochlea $\hat{Z}_{\text{SC}}$. Although the two-port network, and thus $\hat{Z}_{\text{TOC}}$, could depend on the state of the TM (e.g., normal versus perforated) and the perforation characteristics (e.g., location and size), our measurements show that $\hat{Z}_{\text{TOC}}$ is not much affected by perforations (Voss *et al.*, 2001d, Fig. 4),[1] thus supporting the simplification that $\hat{Z}_{\text{TOC}}$ is independent of perforations. Measurements also support the assumption that $\hat{Z}_{\text{perf}}$ does not depend on perforation location (Voss, 1998; Voss *et al.*, 2000c).

One prediction of the circuit topology has been tested. In the circuit, the magnitude of the impedance at the TM, $|\hat{Z}_{\text{TM}}|$, has a minimum at frequencies where the magnitude of the pressure-difference ratio

$$|\hat{H}_{\Delta\text{TM}}| \equiv \left| \frac{(\hat{P}_{\text{TM}} - \hat{P}_{\text{cav}})}{\hat{P}_{\text{TM}}} \right|, \tag{1}$$

is a maximum. Specifically, the circuit requires that

$$\hat{H}_{\Delta\text{TM}} = \frac{\hat{Z}_{\text{perf}} \| \hat{Z}_{\text{TOC}}}{\hat{Z}_{\text{TM}}}. \tag{2}$$

Equation (3) predicts that local maxima in $|H_{\Delta\text{TM}}|$ will occur at the frequencies of local minima in $|Z_{\text{TM}}|$. Figure 6 of the companion paper (Voss *et al.*, 2001d) shows that our data fit this prediction over 53 perforation conditions in ten ears.

B. Representation of model components

A model was constructed for each of ten ears from measurements on that ear along with a $\hat{Z}_{\text{perf}}$ (as a function of frequency and perforation diameter) based on a theoretical model supported by independent acoustic measurements. The ten ears are the ten human-cadaver ears on which impedance measurements were made (Voss *et al.*, 2001d; Voss, 1998). Superscripts norm and perf designate the normal and perforated states of the TM, respectively.

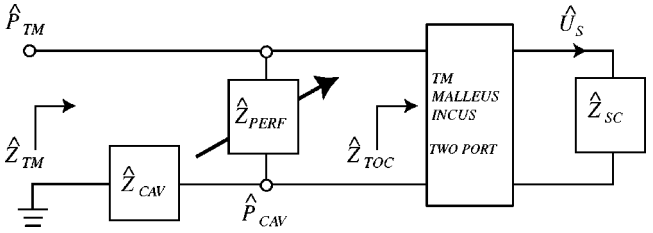

FIG. 1. Model of the human middle ear with a perforation. Voltages are analogous to sound pressures; nodes in the circuit are labeled with symbols for sound pressures, e.g., $\hat{P}_{\text{cav}}$. Currents are analogous to volume velocities; arrows on branches are labeled with volume-velocity symbols, e.g., $\hat{U}_S$. To distinguish them from measurements, model components are indicated with a circumflex to distinguish them from measured values. The TM, malleus, incus two-port network represents tympanic–membrane–ossicular coupling through the TM to the stapes and cochlea. $\hat{Z}_{\text{SC}}$ is the net impedance of the cochlea and the stapes. The input impedance $\hat{Z}_{\text{TOC}}$ of the two-port network (terminated by $\hat{Z}_{\text{SC}}$) is identical for the normal and perforated conditions. $\hat{Z}_{\text{cav}}$ is the impedance of the middle-ear cavity; $\hat{P}_{\text{TM}}$ is the sound pressure at the TM; $\hat{P}_{\text{cav}}$ is the sound pressure in the middle-ear cavity; $\hat{U}_S$ is the stapes volume velocity; and $\hat{Z}_{\text{perf}}$ is the impedance of a perforation. The arrow through $\hat{Z}_{\text{perf}}$ indicates that $\hat{Z}_{\text{perf}}$ depends on perforation size. The input impedance at the TM is $\hat{Z}_{\text{TM}}$.

In the individual-ear models used in this section, impedance measurements (Voss *et al.*, 2001d) directly determine each model middle-ear cavity impedance, i.e., $\hat{Z}_{\text{cav}} = Z_{\text{cav}}$ is taken from the measurement of cavity impedance in that ear. $\hat{Z}_{\text{TOC}}$ is obtained from measurements of Z_{cav} and $Z_{\text{TM}}^{\text{norm}}$. With a normal TM (i.e., $|\hat{Z}_{\text{perf}}| = \infty$), the model of Fig. 1 requires that

$$\hat{Z}_{\text{TOC}} = Z_{\text{TM}}^{\text{norm}} - Z_{\text{cav}}. \tag{3}$$

Therefore, for each ear's model, we determine $\hat{Z}_{\text{TOC}} \equiv Z_{\text{TM}}^{\text{norm}} - Z_{\text{cav}}$. Thus, $\hat{Z}_{\text{TM}} \equiv Z_{\text{TM}}$ for each ear.

Measurements of $Z_{\text{TM}}^{\text{norm}}$ and Z_{cav} and computations of $\hat{Z}_{\text{TOC}}$ are shown for the ten ears in Fig. 2. For most frequencies, $|Z_{\text{TM}}^{\text{norm}}| > 5 \times |Z_{\text{cav}}|$, and thus $\hat{Z}_{\text{TOC}} \approx Z_{\text{TM}}^{\text{norm}}$. This use of measurements to represent components of the model allows the analysis of the model to test the adequacy of the circuit topology for representing measurements with perforations.

To specify $\hat{Z}_{\text{perf}}$, we represent the perforation as a circular orifice in a thin plate. No theoretical derivation for the impedance of a circular orifice with dimensions that correspond to the thickness of the TM of 0.06 mm (Lim, 1995) and perforations on the order of 0.5–5 mm in diameter has been agreed upon (e.g., Sivian, 1935; Bolt *et al.*, 1949; Ingård and Labate, 1950; Kuckes and Ingård, 1953; Nolle, 1953; Thurston and Martin, 1953; Stinson and Shaw, 1985). However, Stinson and Shaw (1985) report measurements of the impedance of circular orifices in thin plates that are of comparable dimensions to our smaller perforations. Furthermore, they show that their measured impedances are in excellent agreement with expressions suggested by Thurston (1952), in which the impedance of a circular orifice is approximated by the input impedance of a cylindrical tube (''shorted'' at its other end) with a length that is extended by two ''end corrections.'' Applied to the perforations, the description is

$$\hat{Z}_{\text{perf}} = \frac{4\rho 2\pi f(t+\delta)}{\pi d^2}\phi, \tag{4}$$

where

$$\phi \equiv -j\frac{J_0(\kappa d/2)}{J_2(\kappa d/2)} \tag{5}$$

and f is frequency, $j=\sqrt{-1}$, d is the perforation diameter, ρ is the density of air, $t=0.06$ mm is the thickness of the TM (Lim, 1995), $\delta=8d/3\pi$, $\kappa^2=-j\rho 2\pi f/\mu$ where μ is the coefficient of viscosity of air ($\mu=1.82\times10^{-5}\,\text{kg s}^{-1}\,\text{m}^{-1}$), and J_0 and J_2 are zero- and second-order Bessel functions (of complex arguments), respectively.

Figure 3 shows, as a function of frequency, both the factor ϕ and the impedance $\hat{Z}_{\text{perf}}$, with perforation diameter as the parameter. At the lower frequencies, for the smaller perforations, ϕ varies substantially with frequency (in magnitude and angle) and the perforation impedance $\hat{Z}_{\text{perf}}$ has comparable resistive and mass components. As the perforation diameter increases, $|\phi|\rightarrow 1$ and $\angle\phi\rightarrow 0.25$, and the impedance becomes mass dominated. As frequency increases above 1000 Hz, for all diameters, $|\phi|\rightarrow 1$ and $\angle\phi\rightarrow 0.25$, and the impedance is mass dominated; for this range $|\hat{Z}_{\text{perf}}|$ is approximately inversely proportional to diameter.

One assumption inherent in our use of this model for $\hat{Z}_{\text{perf}}$ involves the relative velocities of the TM and the air moving through the perforation. The model is a circular orifice in a stationary baffle, whereas the TM is a membrane that vibrates. Our measurements, however, indicate that for perforations that include up to at least 25% of the TM, the TM velocity is generally at least ten times smaller than the particle velocity of air flowing through the perforation;[2] thus the model's assumption that the TM's velocity is small relative to the particle velocity of air moving through the perforation is accurate.

III. COMPARISON OF MODEL PREDICTIONS TO MEASUREMENTS

A. Organization

In general, the figures in this section compare the model to the measurements for one ear (Bone 24L) as a typical example. [Comparisons for all other ears are similar and can be found in the appendices of Voss (1998).[3]]

We start by comparing impedance at the TM with perforations (Sec. III B). Because the model is based on bone-specific measurements except for the impedance of the perforation, similarity between measurements and model

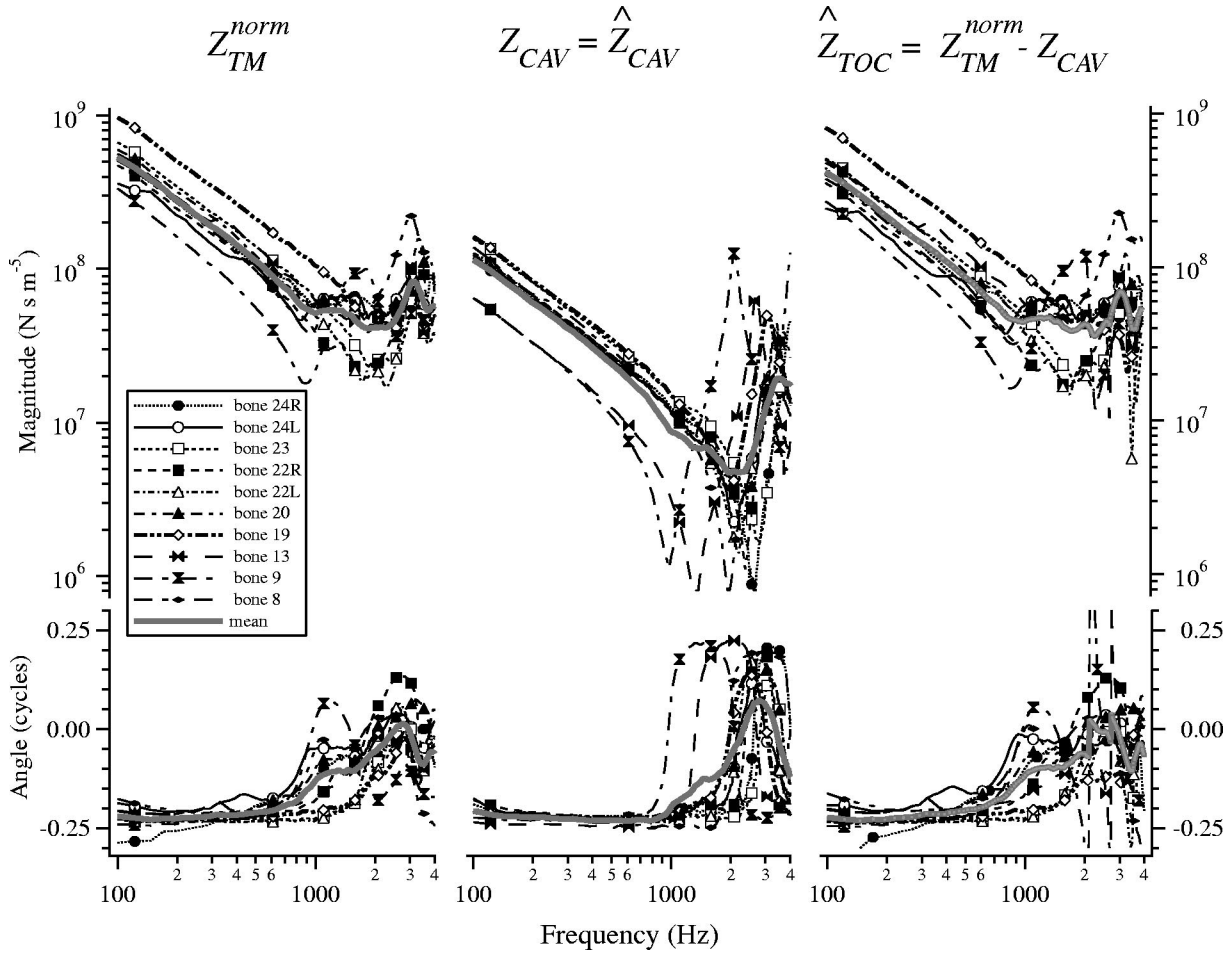

FIG. 2. Impedances from ten temporal-bone preparations as used to specify components in models for each ear. Left: Impedance measured at the normal TM, $Z_{\text{TM}}^{\text{norm}}$. Middle: Impedance measured with the TM removed Z_{cav}. Right: Impedance $\hat{Z}_{\text{TOC}}$ calculated from measurements as $\hat{Z}_{\text{TOC}}=Z_{\text{TM}}^{\text{norm}}-Z_{\text{cav}}$. Upper panel: Magnitude. The magnitude means were computed in the logarithmic domain. Lower panel: Angle. The equations at the tops of the three columns indicate how the measurements are used to determine each model's components. Symbols indicate every 20th point.

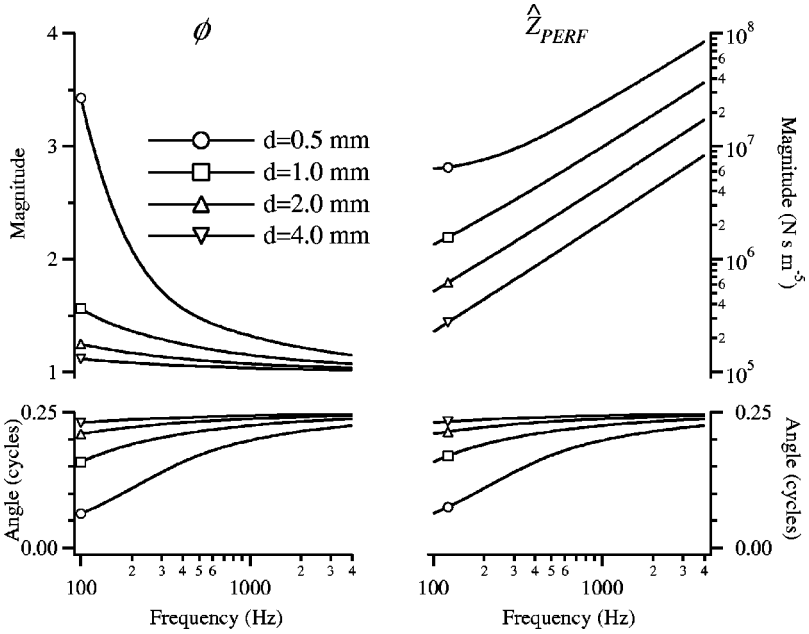

FIG. 3. Values of ϕ [Eq. (5)] and $\hat{Z}_{\text{perf}}$ [Eq. (4)]. The parameter d is perforation diameter.

indicates that (1) the inclusion of $\hat{Z}_{\text{perf}}$ in the model produces the measured effects of perforations and (2) the model for $\hat{Z}_{\text{perf}}$ is consistent with the measurements.

Next, in Sec. III C, we compare perforation-induced changes in (1) stapes velocity and (2) pressure differences across the TM. In this section, the data that are compared to the model were not used in any way to define the model parameters.

B. Impedance at the tympanic membrane

Figure 4 compares model and measurements for one ear (Bone 24L). All of the salient features of the measurements are seen in the model's behavior: (1) At the lower frequencies, the model and the measurements have similar magnitudes and decrease at 20 dB/decade with an angle that is approximately -0.20 cycles, (2) in both model and measurements the angle changes from negative to positive at a perforation-diameter-dependent frequency that varies from 700 Hz for the smallest perforation to 2000 Hz for the largest; (3) both model and measurements have a magnitude minimum whose frequency increases with increasing perforation diameter, and (4) near 3000 Hz, the model and the measurements have similar local magnitude maxima which decreases as perforation diameter increases. The similarity between the measured $Z_{\text{TM}}^{\text{perf}}$ and the model $\hat{Z}_{\text{TM}}^{\text{perf}}$ shows that the model for $\hat{Z}_{\text{perf}}$ [i.e., Eq. (4)] provides an accurate representation of the perforation's effects on input impedance for the entire frequency range and span of perforation diameters.

C. Transmission loss

With values for $\hat{Z}_{\text{TOC}}$, $\hat{Z}_{\text{perf}}$, and $\hat{Z}_{\text{cav}}$, we use the model of Fig. 1 to predict loss in sound transmission caused by perforations. The model's perforation-induced change in transmission (i.e., loss), $\Delta\hat{T}$, can be expressed as either (1) the ratio between the volume velocity through the element $\hat{Z}_{\text{SC}}$ with a normal TM and the volume velocity through the element $\hat{Z}_{\text{SC}}$ with a perforated TM or (2) the ratio between the pressure-difference transfer function [i.e., Eq. (2)] across

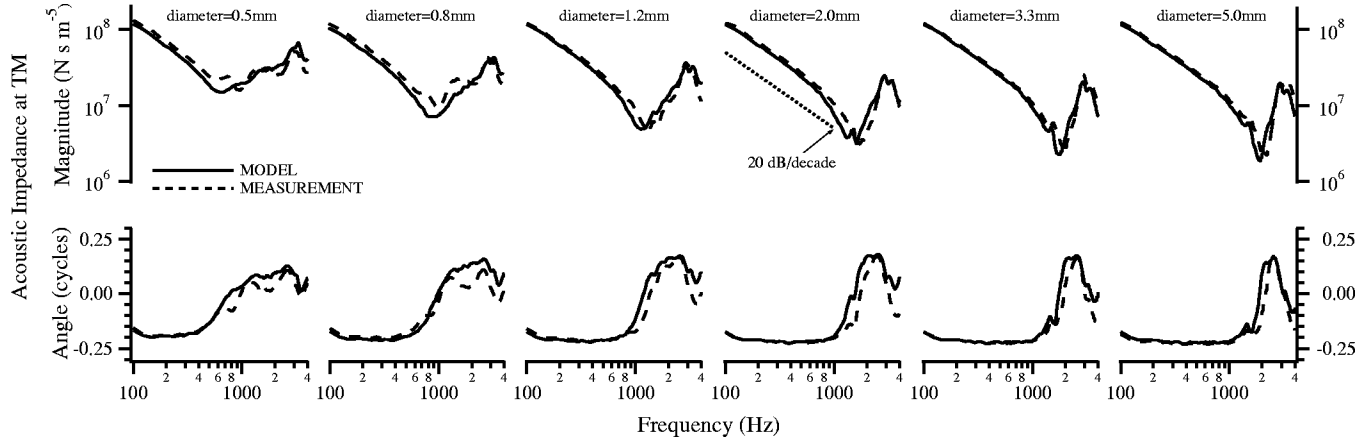

FIG. 4. Comparisons of the measured impedance at the TM $Z_{\text{TM}}^{\text{perf}}$ to the model prediction of impedance at the TM $\hat{Z}_{\text{TM}}^{\text{perf}}$ for six perforation diameters. Upper panel: Magnitudes. Lower panel: Angles. Note: The "normal" (no perforation) condition is not shown as the model is identical to the measurements by definition.

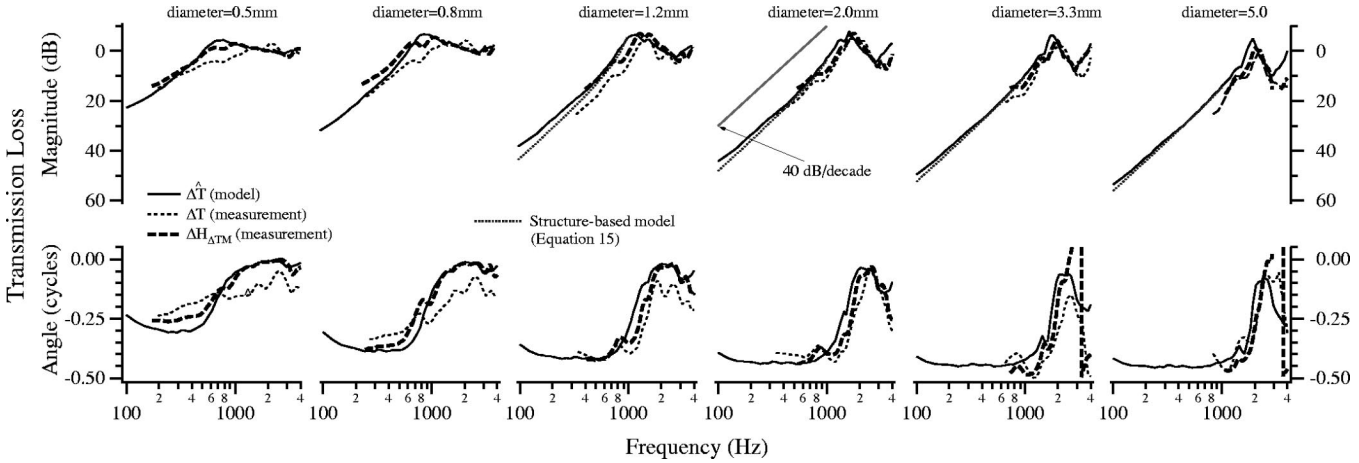

FIG. 5. Model and measurements of perforation-induced loss in transmission. The model (solid lines) is from Eq. (6) with the magnitude expressed in dB as $20\log_{10}|\Delta\hat{T}|$. Measurements from Voss *et al.* (2001d) are changes from normal in both stapes velocity $\Delta V_S/P_{\mathrm{TM}}$ (thin dashed lines) and pressure difference across the TM $\Delta H_{\Delta\mathrm{TM}}$ (thick dashed lines). Each column corresponds to the indicated perforation diameter. For perforations greater than 1 mm in diameter, the magnitude of the model simplification given by Eq. (12) is indicated by a dotted line which is hard to see in the larger perforations because it is obscured by the ''model''. Upper panel: Magnitudes. Lower panel: Angles.

the TM with a normal TM and the pressure-difference transfer function across the TM with a perforated TM: the two are identical because the only mechanism for perforation-induced change in the model is via the pressure difference across the TM,

$$\Delta\hat{T} \equiv \text{model transmission loss} \equiv \frac{\hat{U}_S^{\mathrm{norm}}}{\hat{U}_S^{\mathrm{perf}}} \equiv \frac{\hat{H}_{\Delta\mathrm{TM}}^{\mathrm{norm}}}{\hat{H}_{\Delta\mathrm{TM}}^{\mathrm{perf}}} \equiv 1 + \frac{\hat{Z}_{\mathrm{cav}} \| \hat{Z}_{\mathrm{TOC}}}{\hat{Z}_{\mathrm{perf}}}, \tag{6}$$

where the loss magnitude in dB equals $20\times\log_{10}(|\Delta\hat{T}|)$. Superimposed plots of the experimentally measured losses [i.e., perforation-induced changes in both stapes velocity and the pressure-difference transfer function (Voss *et al.*, 2001d, Fig. 3 ratio of perforated to normal)] and the model loss [$\Delta\hat{T}$, Eq. (6)] for the example ear can be compared in Fig. 5. Differences between the two measured losses are the measured loss in H_{TOC}, which is much less than the total loss for many conditions.

From Fig. 5 it is clear that the characteristics of the experimental data are present in the model: (1) At the lowest frequency, the loss magnitudes are greatest and they decrease with increasing frequency at about 40 dB/decade, (2) the magnitude of the loss at the lowest frequency increases with increasing perforation diameter, (3) small increases (negative loss magnitudes) in transmission occur around 1000 Hz, and (4) loss magnitudes in the 3000–4000 Hz region increase with perforation diameter. The lower plots (Fig. 5) show the angles of the model and measured losses. Again, many features of the measurements are seen in the model's behavior: (1) For low frequencies, the angle difference is negative (between -0.25 and -0.50 cycles) and relatively flat; thus, the perforations introduces a lag in the transmission. (2) The low-frequency angle becomes more negative as perforation diameter increases, and (3) the angle difference increases toward zero above 1000 Hz and decreases again around 4000 Hz. The model's prediction of transmission loss is not limited by the mechanical artifact, so $\Delta\hat{T}$ can be predicted for the lowest frequencies. For the larger perforations, the model predicts loss that exceeds 50 dB at the lower frequencies.

In summary, the model of Fig. 1 represents changes in sound transmission with perforations quite accurately and provides predictions beyond the range of the measurements. The results demonstrate that the model of Fig. 1 is a useful representation of sound transmission with perforations.

IV. APPLICATIONS OF THE MODEL TO PREDICTION OF HEARING LOSS

A. Goal

As discussed in the companion paper (Voss *et al.*, 2001d), a theory for middle-ear function with perforations can help physicians (1) determine whether a specific hearing loss results only from a perforation or whether other middle-ear pathology should be expected and (2) understand why similar-appearing perforations often result in different hearing losses. This section describes the model's prediction for transmission dependence on frequency, middle-ear cavity volume, and perforation diameter.

B. Dependence on middle-ear cavity volume

The impedance of the middle-ear cavity is an important part of the model for the perforated middle ear. A problem in applying this model of cadaver ears to live ears results from differences between the middle-ear cavities of cadaver and live ears. The measurements (Voss *et al.*, 2001d) were made on ears with middle-ear cavity volumes that were smaller than normal, because it is not possible to retain the entire mastoid cavity when the ear is removed from the cadaver. (The middle-ear cavity volume is the sum of the tympanic-cavity volume and the mastoid cavity volume. The tympanic-cavity volume, which is typically about 1 cm^3 and shows little inter-ear variation, is not affected by the removal process.) The volume of the middle-ear space inferred from acoustic measurements in the cadaver ears ranged from 1.5 to 3.5 cm^3, whereas volumes in normal ears range from 2 to

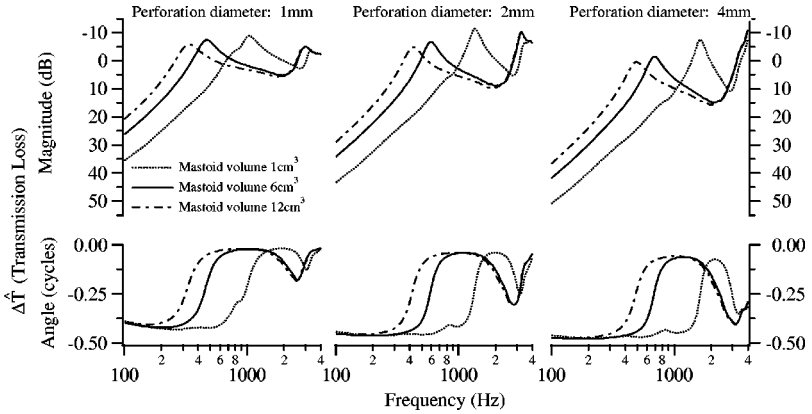

FIG. 6. Model calculations for $\Delta\hat{T}$ with variation of mastoid-cavity volume (1, 6, and 12 cm^3) and perforation diameter (1, 2, and 4 mm). The calculations use Fig. 1 with $\hat{Z}_{\mathrm{TOC}}$ calculated by Eq. (3) from measurements on "Bone 24L", $\hat{Z}_{\mathrm{perf}}$ from Eq. (4), and $\hat{Z}_{\mathrm{cav}} \equiv \hat{Z}_{\mathrm{cav}}^{\mathrm{SB}}$ with $\hat{Z}_{\mathrm{cav}}^{\mathrm{SB}}$ from Voss *et al.* (2000a) with the mastoid-cavity volume having one of three indicated values. See Voss *et al.* (2000b, Fig. 12 and Table I) for details of the calculation of $\hat{Z}_{\mathrm{cav}}^{\mathrm{SB}}$; all element values were held constant except for the mastoid-cavity volume V_a. At frequencies above 2000 Hz, the curves for 6 and 12 cm^3 are essentially indistinguishable.

22 cm^3 (Molvaer *et al.*, 1978). To represent the effects of the smaller-than-normal middle-ear cavity volumes, we introduce a structure-based four-element acoustic model for the middle-ear cavity in which the mastoid-cavity volume is a parameter (Voss *et al.*, 2000b). $\hat{Z}_{\mathrm{cav}}$ (in Fig. 1) is then the structure-based (SB) cavity impedance $\hat{Z}_{\mathrm{cav}}^{\mathrm{SB}}$ with a variable mastoid-cavity volume, i.e.,

$$\hat{Z}_{\mathrm{cav}} \equiv \text{structure-based model} \equiv \hat{Z}_{\mathrm{cav}}^{\mathrm{SB}}. \tag{7}$$

Figure 6 shows how variation in mastoid-cavity volume affects the model prediction for transmission loss $\Delta\hat{T}$. For low frequencies, loss decreases as the mastoid volume increases. Variations of more than 20 dB occur in $|\Delta\hat{T}|$ when the mastoid-cavity volume is varied across the range of volumes found in normal ears (Molvaer *et al.*, 1978). Additionally, the frequency where the loss is a minimum (peak in Fig. 6) decreases as volume increases. These model results illustrate that identical perforations may not lead to similar hearing loss; the middle-ear cavity's mastoid volume plays an important role in determining hearing loss.

C. Low-frequency loss: Dependence on structure

At the lowest frequencies, Eq. (6) for $\Delta\hat{T}$ can be simplified to an analytic expression that describes how $\Delta\hat{T}$ depends on structure at low frequencies. At frequencies where $|\hat{Z}_{\mathrm{cav}}| \ll |\hat{Z}_{\mathrm{TOC}}|$ ($f < 1000$ Hz as in Fig. 2), Eq. (6) can be approximated as

$$\Delta\hat{T} \approx 1 + \frac{\hat{Z}_{\mathrm{cav}}}{\hat{Z}_{\mathrm{perf}}}. \tag{8}$$

Additionally, at the lowest frequencies, $\hat{Z}_{\mathrm{cav}}$ is compliance dominated so that the structure-based cavity impedance $\hat{Z}_{\mathrm{cav}}^{\mathrm{SB}}$ can be approximated as

$$\hat{Z}_{\mathrm{cav}}^{\mathrm{SB}} \approx \frac{\rho c^2}{j2\pi f V}, \quad f < f_c, \tag{9}$$

where V is the total volume of the middle-ear cavity (the sum of the mastoid-cavity and tympanic-cavity volumes) and f_c is a frequency limit above which $\hat{Z}_{\mathrm{cav}}^{\mathrm{SB}}$ cannot be approximated by a compliance. The frequency f_c depends on V. As discussed in Voss *et al.* (2000b), the tympanic-cavity volume does not vary much from about 1 cm^3 across all ears, but the mastoid-cavity volume shows substantial variation (i.e., an order of magnitude). Because of the acoustic interaction of the two volumes (i.e., the tympanic-cavity volume and the mastoid-cavity volume), f_c decreases as V increases. For mastoid-cavity volume V_a such that $V_a < 2$ cm^3, $f_c \approx 1000$ Hz; for $V_a = 6$ cm^3, $f_c \approx 500$ Hz; and for $V_a = 12$ cm^3, $f_c \approx 250$ Hz. [See Fig. 13 of Voss *et al.* (2000b) for the specific dependence of $\hat{Z}_{\mathrm{cav}}^{\mathrm{SB}}$ on mastoid-cavity volume.]

For the larger perforations (i.e., $d > 1$ mm) $\hat{Z}_{\mathrm{perf}}$ is mass dominated (Fig. 3) so that

$$\hat{Z}_{\mathrm{perf}} \approx j2\pi f \hat{M}_{\mathrm{perf}}, \quad d > 1 \text{ mm} \tag{10}$$

and

$$\hat{M}_{\mathrm{perf}} \approx \frac{4\rho}{\pi d^2}\frac{8d}{3\pi}1.2, \tag{11}$$

where the term $(t+\delta)$ from Eq. (4) is approximated by $\delta = 8d/3\pi$ [since $\delta \gg t$], and the term ϕ in Eq. (4) is approximated by the constant 1.2. [The term ϕ—defined in Eq. (5)—is frequency dependent. As either perforation diameter or frequency increases, $|\phi| \to 1$ and $\angle\phi \to 0.25$ cycles (Fig. 3). We have approximated $|\phi|$ by 1.2, as 1.2 is a middle value of the total range that $|\phi|$ covers for the frequencies and perforation diameters of interest.]

Substitution of Eq. (9) and (10) into Eq. (8) leads to the approximation

$$\Delta\hat{T} \approx 1 - \frac{\alpha d}{f^2 V}, \quad f < f_c, \tag{12}$$

where $\alpha = 2.3 \times 10^6$ $cm^3/mm\,s^2$, diameter d has units mm and $d > 1$ mm, middle-ear cavity volume V has units cm^3, and frequency f has units Hz with Eq. (12) valid for frequencies where $\hat{Z}_{\mathrm{cav}}$ is compliance dominated (i.e., $f < f_c$). The magnitude $|\Delta\hat{T}|$ predicted with the approximation of Eq. (12) is plotted in Fig. 5 for perforations with diameters greater than 1 mm, and differences between this approximation and $|\Delta\hat{T}|$ from the complete model of Eq. (6) are minimal. Thus, Eq. (12) approximates $\Delta\hat{T}$ [Eq. (6)] for frequencies below 500 Hz (with total cavity volume V of about 2 cm^3) and perforation diameters greater than 1 mm.

The accuracy of Eq. (12) in predicting the measured loss can be tested with data reported in the companion paper (Voss *et al.*, 2001d). Figure 7 shows results for a frequency of 680 Hz, which is below the $f_c = 1000$ Hz appropriate for

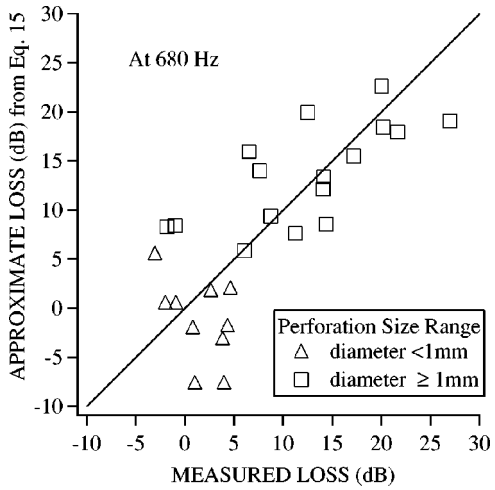

FIG. 7. A scatter plot of the measured perforation-induced transmission loss from the companion paper (Voss *et al.*, 2001d) vs the model-based approximation [Eq. (12)] at 680 Hz. The line indicates $y=x$. The plotted points correspond to all the measurements in which transmission loss at 680 Hz was accurately determined and the impedance measurements existed. The data include 26 perforations in 7 ears.

the volumes of the modified cadaver ears (range of 1.3 to 1.7 cm^3). The plot indicates that the approximate expression is consistent with the large trend in the measurements. The largest deviations from perfect prediction (the line in Fig. 7) are about 10 dB and the root-mean square error between predicted and measured is 5.9 dB. The errors for cases of small perforation are similar to those with larger perforations; an explanation for this is that for the frequency illustrated (680 Hz) the model for the perforation impedance (see Fig. 3) roughly satisfies the mass-like assumption of the approximation for all perforations larger than 0.4 mm in diameter. Figure 7 supports the use of Eq. (12) to estimate transmission loss, although it does not test the dependence of the loss on middle-ear volume, as the volumes in these ears are all within ± 0.2 cm^3 of 1.5 cm^3.

The approximation [Eq. (12)] may be useful clinically to estimate the effects of an existing perforation on hearing loss. Middle-ear cavity volume could be estimated via low-frequency impedance measurements, which will also determine the frequency range in which the approximation is expected to be accurate. For a particular ear, estimation of hearing loss caused by the perforation should allow clinicians to estimate the loss caused by other pathologies.

D. Future clinical studies of hearing with perforations

The theory presented here, coupled with the companion paper (Voss *et al.*, 2001d), provide a basis for future clinical studies of hearing with perforations. In particular, this work identifies the middle-ear cavity volume as an important variable in hearing with perforations. In future studies, the middle-ear cavity volume can be estimated via either low-frequency impedance measurements or CT scans (or a combination of the two). Additionally, future studies that rely on audiometrically measured hearing levels should include measurements of the sound pressure levels generated by the earphone in the ear canal, as recent measurements have shown that ears with lower-than-normal input impedances can reduce the ear-canal sound pressure relative to that produced in the ear canal of an ear with a normal input impedance (Voss *et al.*, 2000a,e).

V. CONCLUSIONS

A simple model for sound transmission with perforations in the tympanic membrane is tested. The perforation is represented by an impedance, which depends on frequency and perforation diameter, and is between the ear canal and the middle-ear cavity. The model's predictions for the input impedance of the middle ear and the transmission loss to the cochlea are similar to measurements of these quantities (Voss *et al.*, 2001d). Modification of the model to allow middle-ear cavity volume to be a parameter predicts that variations in middle-ear cavity volume can result in variations in hearing loss of up to 20 dB. Simplification of the model to a structure-based expression for low frequencies and perforation diameters greater than 1 mm should be useful to clinicians in relating hearing losses with perforation size, frequency, and cavity volume.

ACKNOWLEDGMENTS

This work was supported by training and research grants from the NIDCD. We thank Douglas H. Keefe of the Physical Acoustics Lab at the Boys Town National Research Hospital, Christopher Shera of the Eaton Peabody Laboratory at the Massachusetts Eye and Ear Infirmary, and Michael R. Stinson of the National Research Council (Ottawa, Canada) for helpful discussions. We also thank two JASA reviewers, Dr. Robert H. Margolis and an anonymous reviewer, for helpful suggestions.

[1]To see how Voss *et al.* (2001d, Fig. 4) support the statement that $\hat{Z}_{TOC}$ is not (much) affected by perforations, consider the transfer admittance of the two-port network of Fig. 1:

$$\hat{G}_{TOC} \equiv \frac{\hat{U}_S}{\hat{P}_{TM}-\hat{P}_{cav}} = \frac{\hat{\alpha}\hat{V}_S}{\hat{P}_{TM}-\hat{P}_{cav}} = \hat{\alpha}\hat{H}_{TOC}, \tag{13}$$

where the model's stapes volume velocity $\hat{U}_S$ is related to the model's stapes velocity $\hat{V}_S$ via $\hat{\alpha}$, which might depend on both frequency and perforation characteristics. The companion paper (Voss *et al.*, 2001d) discusses measurements of the transfer function $H_{TOC}=V_S/(P_{TM}-P_{cav})$, which in the model is $\hat{G}_{TOC}/\hat{\alpha}$. The measurements show that H_{TOC} is not a strong function of TM state. Specifically, measurements of $|H_{TOC}|$ with perforations that cover up to 25% of the TM are within 5 dB of $|H_{TOC}|$ measured with a normal TM; also, measurements show that changes from normal in $\angle H_{TOC}$ are generally less than 0.05 cycles. Measurements also support the assumption that $\hat{\alpha}$ does not depend strongly on TM state. Specifically, velocity measurements made at several locations on the stapes' suprastructure show that character of the stapes motion is not affected by perforations; the stapes primarily translates in one direction for both normal and perforated TMs up to at least 2000 Hz (e.g., Voss *et al.*, 2000b, 2001d; Voss, 1998). This experimental finding supports the assumption that $\hat{\alpha}$ does not depend on the state of the TM. In summary, our model assumption that $\hat{Z}_{TOC}$ is independent of the state of the TM is supported through measurements that show (1) H_{TOC} does not depend strongly on perforation state and (2) the mode of stapes motion is not affected by perforations.

[2]The two relevant velocities were estimated from measurements: (1) the TM velocity V_{TM} and (2) the particle velocity of air flowing through the perforation (V_{perf});

$$V_{TM}=\frac{P_{TM}}{Z_{TM}A_{TM}}, \tag{14}$$

where $A_{TM}=70$ mm^2 is the TM area (Wever and Lawrence, 1954), and

$$V_{perf}=\frac{P_{TM}-P_{cav}}{Z_{perf}A_{perf}}, \tag{15}$$

where A_{perf} is the measured cross-sectional area of the perforation. Estimates of the velocity magnitudes $|V_{TM}|$ and $|V_{perf}|$ from one of our ears are plotted in Fig. 4–5 of Voss (1998). We note that for perforation diameters of 3.3 and 5.0 mm, $|V_{TM}|$ approaches $|V_{perf}|$ for substantial frequency ranges above 800 Hz; however, $|V_{TM}|$ is generally less than $|V_{perf}|$.

[3]The model description of $\hat{Z}_{perf}$ in Voss (1998) is not identical to that used here; however, differences between the predictions from the two models are negligible.

Bolt, R. H., Labate, S., and Ingård, U. (**1949**). ''The acoustic reactance of small circular orifices,'' J. Acoust. Soc. Am. **21**, 94–97.

Ingård, U., and Labate, S. (**1950**). ''Acoustic circulation effects and the nonlinear impedance of orifices,'' J. Acoust. Soc. Am. **22**, 211–218.

Kringlebotn, M. (**1988**). ''Network model for the human middle ear,'' Scand. Audiol. **17**, 75–85.

Kuckes, A., and Ingård, U. (**1953**). ''Letter to the editor: A note on acoustic boundary dissipation due to viscosity,'' J. Acoust. Soc. Am. **25**, 798–799.

Lim, D. (**1995**). ''Structure and function of the tympanic membrane: A review,'' Acta otorhino-laryngologica Belg. **49**, 101–115.

Møller, A. R. (**1961**). ''Network model of the middle ear,'' J. Acoust. Soc. Am. **33**, 168–176.

Molvaer, O., Vallersnes, F., and Kringlebotn, M. (**1978**). ''The size of the middle ear and the mastoid air cell,'' Acta Oto-Laryngol. **85**, 24–32.

Nolle, A. (**1953**). ''Small-signal impedance of short tubes,'' J. Acoust. Soc. Am. **25**, 32–39.

Onchi, Y. (**1961**). ''Mechanism of the middle ear,'' J. Acoust. Soc. Am. **33**, 794–805.

Peake, W., Rosowski, J. J., and Lynch, T. J. (**1992**). ''Middle-ear transmission: Acoustic versus ossicular coupling in cat and human,'' Hear. Res. **57**, 245–268.

Shera, C. A., and Zweig, G. (**1992**). ''Middle-ear phenomenology: The view from the three windows,'' J. Acoust. Soc. Am. **92**, 1356–1370.

Sivian, L. (**1935**). ''Acoustic impedance of small orifices,'' J. Acoust. Soc. Am. **7**, 94–101.

Stinson, M. R., and Shaw, E. (**1985**). ''Acoustic impedance of small, circular orifices in thin plates,'' J. Acoust. Soc. Am. **77**, 2039–2042.

Thurston, G. B. (**1952**). ''Periodic fluid flow through circular tubes,'' J. Acoust. Soc. Am. **24**, 653–656.

Thurston, G. B., and Martin, Jr., C. E. (**1953**). ''Periodic fluid flow through circular orifices,'' J. Acoust. Soc. Am. **25**, 26–31.

Voss, S. E. (**1998**). ''Effects of tympanic-membrane perforations on middle-ear sound transmission: Measurements, mechanisms, and models'' Ph.D. thesis, Massachusetts Institute of Technology.

Voss, S. E., Rosowski, J. J., Merchant, S. N., and Peake, W. T. (**2000b**). ''Acoustic responses of the human middle ear,'' Hear. Res. **150**, 43–69.

Voss, S. E., Rosowski, J. J., Merchant, S. N., and Peake, W. T. (**2000c**). ''How do tympanic-membrane perforations affect human middle-ear sound transmission?'' Acta Oto-Laryngologica (in press).

Voss, S. E., Rosowski, J. J., Merchant, S. N., and Peake, W. T. (**2001d**). ''Measurements and mechanisms of middle-ear function with tympanic-membrane perforations,'' J. Acoust. Soc. Am. **110**, 1432–1444.

Voss, S. E., Rosowski, J. J., Merchant, S. N., Thornton, A. R., Shera, C. A., and Peake, W. T. (**2000e**). ''Middle ear pathology can affect the ear-canal sound pressure generated by audiologic earphones,'' Ear Hear. **21**, 265–274.

Voss, S. E., Rosowski, J. J., Shera, C. A., and Peake, W. T. (**2000a**). ''Acoustic mechanisms that determine the ear-canal sound pressures generated by earphones,'' J. Acoust. Soc. Am. **107**, 1548–1565.

Wever, E. G., and Lawrence, M. (**1954**). *Physiological Acoustics* (Princeton University Press, Princeton).

Whittemore, Jr., K. R., Merchant, S. N., and Rosowski, J. J. (**1998**). ''Acoustic mechanisms: Canal wall-up versus canal wall-down mastoidectomy,'' Otolaryngol.-Head Neck Surg. **118**, 751–761.

Zwislocki, J. (**1962**). ''Analysis of the middle-ear function. 1. Input impedance,'' J. Acoust. Soc. Am. **34**, 1514–1523.